

Fluorite transition metal hydride induced destabilization of the MgH_2 system in $\text{MgH}_2/\text{TMH}_2$ multilayers ($\text{TM}=\text{Sc, Ti, V, Cr, Y, Zr, Nb, La, Hf}$)

S. X. Tao, P. H. L. Notten, R. A. van Santen, and A. P. J. Jansen
*Laboratory of Inorganic Chemistry and Catalysis, Eindhoven University of Technology,
 P.O. Box 513, 5600 MB Eindhoven, The Netherlands*

(Received 21 July 2010; revised manuscript received 31 August 2010; published 28 September 2010)

The structural changes in MgH_2 induced by contact with fluorite transition metal hydrides (TMH_2 , $\text{TM}=\text{Sc, Ti, V, Cr, Y, Zr, Nb, La, Hf}$) have been studied using density-functional theory calculations. Models of MgH_2 (rutile)/ TiH_2 (fluorite) and MgH_2 (fluorite)/ TiH_2 (fluorite) multilayers with different $\text{Mg}:\text{TM}$ ratios have been designed. With a fixed thickness of the TMH_2 layer, structure transformation of MgH_2 from rutile to fluorite occurs with a decrease in thickness of the MgH_2 layer. The hydrogen desorption energy from the fluorite MgH_2 layer in the multilayers is significantly lower than that of the bulk rutile MgH_2 . The structural deformation of the MgH_2 layer due to the strain induced by TMH_2 is found to be responsible for the destabilization of the Mg-H bond: the more structural deformation, the more destabilization of the Mg-H. Our results provide an important insight for the development of new hydrogen-storage materials with desirable thermodynamic properties.

DOI: [10.1103/PhysRevB.82.125448](https://doi.org/10.1103/PhysRevB.82.125448)

PACS number(s): 68.35.Md, 68.65.Ac, 88.30.R-

I. INTRODUCTION

MgH_2 is one of the most attractive hydrogen-storage materials because it is inexpensive and light.¹⁻³ However, the kinetics of the hydrogen uptake and release in Mg are poor, and MgH_2 is too stable, leading to too high desorption temperatures (T_d) at atmospheric pressure. For example, the desorption energy of MgH_2 is 75 kJ/mol ($T_d=300$ °C) (Ref. 4) while a desorption energy of 20–50 kJ/mol ($T_d=20$ –100 °C) is desirable. Destabilization upon reduction in the Mg particle size has been predicted theoretically⁵⁻⁸ and observed experimentally.⁹⁻¹¹ Tuning of the thermodynamics and kinetics of the MgH_2 has also been achieved by means of alloying Mg with a second transition metal ($\text{TM}=\text{Ti, Sc, V, Nb, Mn, Cr, Ni, Fe, Pd}$),¹²⁻²⁸ although this leads to a reduction in the storage capacity.

For the $\text{Mg}_x\text{TM}_{1-x}\text{H}_y$ system, electrochemical measurements revealed that inserting and extracting hydrogen is greatly facilitated when containing more than 20 at. % of TM ($\text{TM}=\text{Sc, Ti, V, Cr}$).¹⁹⁻²¹ X-ray diffraction measurements indicated the presence of face-centered-cubic (fcc) structures of hydride with excellent kinetics, whereas a body-centered tetragonal structure of unalloyed Mg strongly inhibited hydrogen transport.²¹ The fcc structure of $\text{Mg}_x\text{TM}_{1-x}\text{H}_y$ system has been proposed to be responsible for the improved kinetics. This structural transformation from rutile to fluorite by alloying fluorite TMH_2 ($\text{TM}=\text{Sc, Ti, V, Cr, Zr, Hf}$) with MgH_2 was also confirmed by earlier density-functional theory (DFT) calculations.^{29,30} Besides the improved kinetics, Baldi *et al.*^{27,28} managed to tune the thermodynamics of hydrogen absorption in Mg-Ti-Pd system by means of elastic clamping. Their results show that the thermodynamics of hydrogen absorption in Pd-capped Mg films are strongly dependent on the magnesium thickness.²⁷ This dependency can be suppressed by inserting a thin Ti layer between Mg and Pd. Furthermore, Mg/Ti multilayers with various monolayer thicknesses between 0.5 and 20 nm were prepared. The layer thickness dependence of hydrogenation properties was again

reported.²⁸ Beside the elastic clamping effect of the Pd layer, the interface effect was also proposed to be responsible for the different thermodynamics. However, no direct evidence was provided.

Inspired by the above developments, we aim to understand the aspects which were not covered experimentally by DFT studies. For instance, how much does the interface effect contribute to the tuned hydrogen desorption thermodynamics? Is there a structural transformation from rutile to fluorite of the MgH_2 layers in the multilayers? Do all fluorite TMH_2 layers have a similar effect on MgH_2 ? To answer these questions, MgH_2 (rutile)/ TMH_2 (fluorite) and MgH_2 (fluorite)/ TMH_2 (fluorite) multilayers with a fixed thickness of the TMH_2 layer and various thickness of the MgH_2 layer have been designed. The stability of these two structures with different thicknesses of the MgH_2 layer is calculated and compared. This gives an estimate for the crossover points of the structural transformation between the two. In addition, by calculating the hydrogen desorption energies, destabilization of MgH_2 is found in the MgH_2 (fluorite)/ TMH_2 (fluorite) multilayers. The destabilized Mg-H bond provides desirable thermodynamics for hydrogen-storage applications.

II. COMPUTATIONAL METHODS AND STRUCTURAL MODELS

All calculations were performed using DFT as implemented in the Vienna *ab initio* simulation package (VASP).^{31,32} The Kohn-Sham equations were solved using a basis of projector augmented wave functions with a plane-wave energy cutoff of 400 eV (Ref. 33) and using pseudopotentials³⁴ to describe the core electrons. The Perdew-Wang 1991 generalized gradient approximation was used for the electron-exchange-correlation potential.³⁵ A total of $7 \times 7 \times 7$ k points and were used to model the Brillouin zone for the 16 metal supercell. For larger cells k points were scaled down proportionally, e.g., for a lattice parameter of

TABLE I. Structural parameters (in Å) and formation energies (eV/H₂) of metal hydrides. The parameters in parentheses are literature values.

Hydride	Structure type	Cell parameter	Formation energy
MgH ₂	Rutile	$a=4.45(4.50)$ $c=2.99(3.01)$	-0.67
MgH ₂	Fluorite	$a=4.70$	-0.33
ScH ₂	Fluorite	$a=4.74(4.78)$	-2.11
TiH ₂	Fluorite	$a=4.40(4.43)$	-1.55
VH ₂	Fluorite	$a=4.20(4.27)$	-0.72
CrH ₂	Fluorite	$a=4.07(3.86)$	+0.13
YH ₂	Fluorite	$a=5.17(5.20)$	-2.18
ZrH ₂	Fluorite	$a=4.80(4.77)$	-1.71
NbH ₂	Fluorite	$a=4.56(4.57)$	-0.70
LaH ₂	Fluorite	$a=5.62(5.67)$	-2.00
HfH ₂	Fluorite	$a=4.70(4.68)$	-1.49

double length, only half the number of k points were required. For all structures the lattice parameters, the volume, and the atom positions were allowed to relax. Nine fluorite TMH_2 (Ref. 36) ($TM=Sc, Ti, V, Cr, Y, Zr, Nb, La, Hf$) were studied. Validation of the accuracy of the structural parameters of the hydrides is made in Table I. The agreement with the literature values³⁷ is fairly good. Figure 1 shows models of two multilayered structures (a) $MgH_2(rutile)/TMH_2(fluorite)$ and (b) $MgH_2(fluorite)/TMH_2(fluorite)$. In this study the notation “ $x1/4l$ ” is always used to indicate the number of monolayer in MgH_2 ($x1$) and TMH_2 ($4l$) layers. Because rutile MgH_2 (001) and fluorite MgH_2 (100) have similar lattice parameter a (4.45 Å and 4.70 Å, respectively), the two multilayers are built by rutile MgH_2 (001) and fluorite TMH_2 (100), and fluorite MgH_2 (100) and fluorite TMH_2 (100), respectively. Due to the varying lattice parameters of TMH_2 , some approximations had to be made.

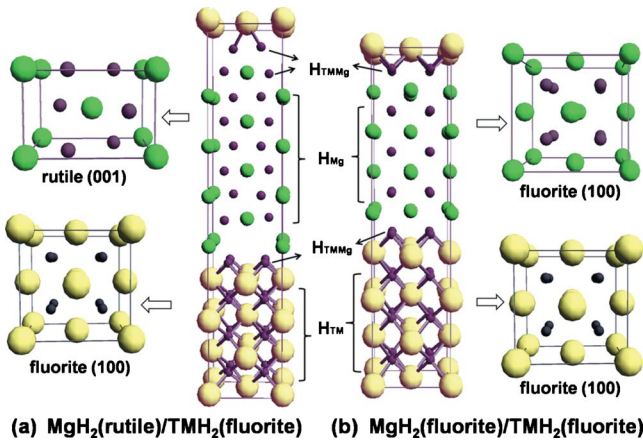


FIG. 1. (Color online) Models of (a) $MgH_2(rutile)/TMH_2(fluorite)$ and (b) $MgH_2(fluorite)/TMH_2(fluorite)$ multilayers with a thickness of $4l/4l$ (four metal atomic layers for fluorite or eight metal atomic layers for rutile). The yellow/light gray, green/gray, and dark gray spheres represent TM , Mg , and H atoms, respectively.

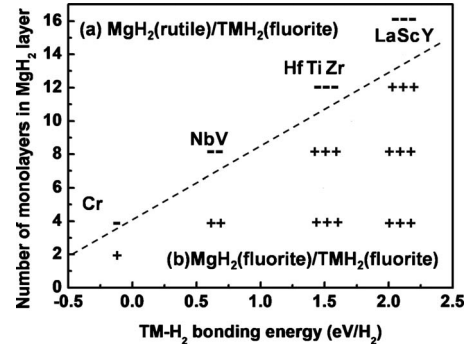


FIG. 2. Relative stability of (a) $MgH_2(rutile)/TMH_2(fluorite)$ and (b) $MgH_2(fluorite)/TMH_2(fluorite)$ as a function of $TM-H_2$ bond energies (in eV/H₂). Total energies of the two structures with the same layer thickness ($x1/4l$) are compared: “+” indicates that (b) is more stable than (a); “-” indicates that (a) is more stable than (b). The dashed line shows the estimated transition point between the two structures.

The same lattice parameter of the MgH_2 [4.70 and 4.45 Å for $MgH_2(rutile)/TMH_2(fluorite)$ and $MgH_2(fluorite)/TMH_2(fluorite)$, respectively] was used also for TMH_2 .

III. STRUCTURAL TRANSFORMATION

The structures and energies of (a) $MgH_2(rutile)/TMH_2(fluorite)$ and (b) $MgH_2(fluorite)/TMH_2(fluorite)$ with a fixed layer thickness of TMH_2 ($4l$) and various layer thicknesses of MgH_2 ($x1$, $0 < x1 \leq 16$) were calculated. The relative stability comparison of the two is depicted in Fig. 2. For instance, for MgH_2/CrH_2 multilayers the structural transformation occurs at MgH_2 layer thickness of $2l < x1 < 4l$, i.e., $MgH_2(fluorite)/CrH_2(fluorite)$ is more stable than $MgH_2(rutile)/CrH_2(fluorite)$ only when MgH_2 layer has a thickness less than $4l$. As one can see, the MgH_2 layer thickness where the transformation of rutile to fluorite occurs is correlated with the bond energy of $TM-H_2$: the larger the bond energy, the thicker the MgH_2 layer. This can be interpreted as that fluorite structure of MgH_2 is a continuation of the TMH_2 due to the induction effect of the strong $TM-H$ bonding at the interfaces. Therefore, this continuation of the fluorite MgH_2 depends highly on how strong the $TM-H$ bonding is. If the $TM-H$ bond is relatively weak, such as, Cr , this continuation is very limited, e.g., only a few atomic layers. In fact, for $MgH_2(fluorite)/TMH_2(fluorite)$, after optimization the fluorite structure of MgH_2 tends to transform into rutile one with the increasing MgH_2 thickness. Beyond a critical thickness of MgH_2 (shown in Fig. 2), the $MgH_2(rutile)/TMH_2(fluorite)$ is more favorable over the $MgH_2(fluorite)/TMH_2(fluorite)$. However, for bulk $Mg_xTM_{1-x}H_2$, there was no such relation. The transformation of rutile to fluorite was calculated at around 20 at. % for Sc, Ti, V , and Cr ,^{29,30} and 13 at. % for Zr and Hf .²⁹ The structural transformation of the MgH_2 layer in the multilayers can also be interpreted as an energy competition between the MgH_2 and the TMH_2 layers. Further evidences will be presented together with the hydrogen desorption energies in the following.

TABLE II. Structures (in Å) and hydrogen desorption energies (in eV/H₂) of (a) MgH₂(rutile)/TMH₂(fluorite) and (b) MgH₂(fluorite)/TMH₂(fluorite) multilayers with thickness 4l/4l. *a* is the lattice parameter in the multilayers plane, *c* is the lattice parameter in the direction perpendicular to the layers.

(a)	<i>a</i> , <i>c</i>	H _{Mg} , H _{TMMg} , H _{TM}
MgH ₂ /ScH ₂	4.68, 21.64	0.98, 1.10, 1.94
MgH ₂ /TiH ₂	4.40, 21.00	0.81, 1.22, 1.23
MgH ₂ /VH ₂	4.32, 20.41	0.78, 1.04, 0.63
MgH ₂ /CrH ₂	4.24, 20.48	0.65, 0.79, -0.11
MgH ₂ /YH ₂	4.87, 22.58	0.92, 1.07, 2.00
MgH ₂ /ZrH ₂	4.60, 22.43	0.86, 1.28, 1.04
MgH ₂ /NbH ₂	4.53, 21.14	0.85, 1.04, 0.34
MgH ₂ /LaH ₂	5.00, 22.50	1.05, 0.69, 1.61
MgH ₂ /HfH ₂	4.50, 22.26	0.78, 1.47, 1.25
(b)	<i>a</i> , <i>c</i>	H _{Mg} , H _{TMMg} , H _{TM}
MgH ₂ /ScH ₂	4.73, 19.10	0.50, 1.12, 2.09
MgH ₂ /TiH ₂	4.61, 16.91	0.44, 1.29, 1.39
MgH ₂ /VH ₂	4.42, 17.67	0.25, 1.17, 0.68
MgH ₂ /CrH ₂	4.31, 17.33	0.21, 0.73, 0.02
MgH ₂ /YH ₂	4.97, 20.08	0.48, 0.95, 2.17
MgH ₂ /ZrH ₂	4.70, 21.85	0.57, 1.22, 1.60
MgH ₂ /NbH ₂	4.61, 18.59	0.48, 0.99, 0.92
MgH ₂ /LaH ₂	5.12, 21.50	0.25, 0.73, 1.89
MgH ₂ /HfH ₂	4.60, 19.57	0.45, 1.37, 1.39

IV. HYDROGEN DESORPTION ENERGY

In the two types of multilayers, three types of hydrogen atoms can be recognized (see Fig. 1) as H_{Mg} (hydrogen occupying Mg layers), H_{TMMg} (hydrogen occupying Mg/TM interfaces), and H_{TM} (hydrogen occupying TM layers). The H_{Mg} desorption energy can be calculated from

$$\Delta E_{H_{Mg}} = E_{MgH_x/TMH_2} + \frac{2-x}{2} E_{H_2} - E_{MgH_2/TMH_2}, \quad (1)$$

where E_{MgH_2/TMH_2} and E_{MgH_x/TMH_2} are the total energy of MgH₂/TMH₂ and MgH_{*x*}/TMH₂ multilayers normalized by

the number of metal atoms. Similar to the H_{Mg} desorption energy, desorption energies of H_{MgTM} and H_{TM} can also be calculated by comparing MgH_{*x*}/TMH₂ to Mg/TMH_{1.5}, Mg/TMH_{1.5} to Mg/TM, respectively.

The calculated hydrogen desorption energies for the two structures with thickness 4l/4l are summarized in Table II. Because of the larger bond energies of TM-H₂ (except for CrH₂) compared to MgH₂ (see Table I), H_{MgTM} and H_{TM} would remain trapped during the desorption process before the desorption of H_{Mg}. Unless the system is heated up, only H_{Mg} absorbs and desorbs reversibly during the hydrogen cycles. Because the more important interest of this study is to seek lower hydrogen desorption energies than that of bulk MgH₂, the desorption of H_{Mg} will be the main focus of this study.

Hydrogen desorption properties of nanoscaled Mg_{*x*}TM_{1-*x*}H_{*y*} are strongly correlated with the structures and compositions.^{26,28} The various hydrogen desorption energies for the two structures are depicted in Fig. 3. H_{Mg} desorption energies from (a) MgH₂(rutile)/TMH₂(fluorite) are always larger than those from (b) MgH₂(fluorite)/TMH₂(fluorite). In addition, when the MgH₂ layer thickness increases from 4l to 8l, the H_{Mg} desorption energy from MgH₂(rutile)/TMH₂(fluorite) decreases while that from MgH₂(fluorite)/TMH₂(fluorite) increases. More interestingly, the H_{Mg} desorption energies from MgH₂(rutile)/TMH₂(fluorite) generally increase with increasing TM-H₂ bond energies. For the ones with relatively high TM-H₂ bond energies, such as, La, Sc, and Y, significant decrease can be observed. This indicates that the thickness of the MgH₂ layer in the multilayers play an important role in changing the thermodynamics of hydrogen desorption, i.e., the thicker the MgH₂ layer, the lower the H_{Mg} desorption energy. It is to be expected that with increasing Mg:TM ratios, the desorption energy has the tendency to converge to the hydrogen desorption energy of rutile MgH₂ (0.67 eV/H₂, see Table I).

In contrast, for MgH₂(fluorite)/TMH₂(fluorite) multilayers, H_{Mg} desorption energy increases (except for Hf where it stays the same) when the MgH₂ layer thickness increases from 4l to 8l. It should be mentioned at this point that when the lattice parameter of TMH₂ is smaller than that of MgH₂, upon forming multilayers the crystal lattice of TMH₂ generally expands while that of MgH₂ compresses, and vice versa. When the lattice parameters of the two are the same or

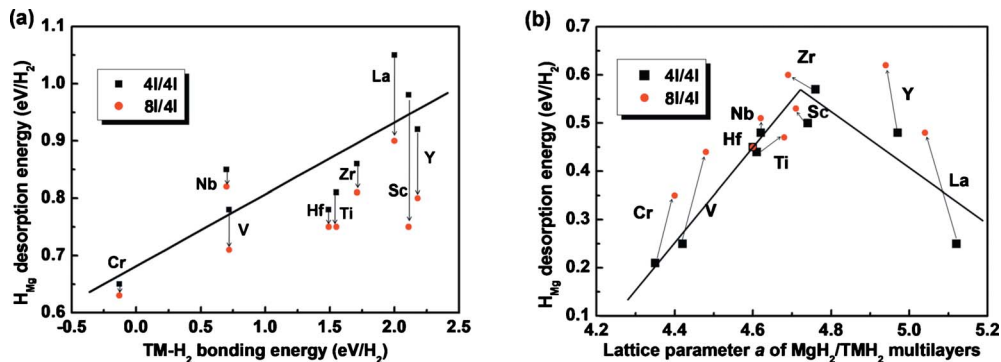


FIG. 3. (Color online) H_{Mg} desorption energies from (a) MgH₂(rutile)/TMH₂(fluorite) as function of TM-H₂ bond energy (in eV/H₂) and from (b) MgH₂(fluorite)/TMH₂(fluorite) as function of lattice parameter *a* (in Å) of the multilayers.

similar, only minor expansion or compression can be observed in lattice a , i.e., $\text{MgH}_2(\text{rutile})/\text{TiH}_2(\text{fluorite})$, and $\text{MgH}_2(\text{fluorite})/\text{ZrH}_2(\text{fluorite})$. This expansion or compression can be observed generally in parameter a . However there are also changes in the lattice c , i.e., the 4% and 11.5% expansion for the $\text{MgH}_2(\text{fluorite})/\text{HfH}_2(\text{fluorite})$ and $\text{MgH}_2(\text{fluorite})/\text{ZrH}_2(\text{fluorite})$, respectively. It is worth noting that the H_{Mg} desorption energies correlate with the lattice parameter a of the multilayers. The crystal-lattice expansion and compression become less when the MgH_2 layer thickness increase from 4l to 8l, thus the H_{Mg} desorption energies increase. Also for each TM , the larger the difference between a of the multilayers and that of MgH_2 , the smaller the desorption energy. For those multilayers with similar lattice parameters to that of MgH_2 , the difference in a between 4l/4l and 4l/8l is minor. Accordingly, the desorption energy does not vary much neither. In fact, for $\text{MgH}_2(\text{fluorite})/\text{HfH}_2(\text{fluorite})$ both the lattice parameters and hydrogen desorption energies remain the same. In conclusion, we can confirm that the crystal-lattice deformation of the multilayers, especially that of the MgH_2 layer, is responsible for the lower H_{Mg} desorption energy. Despite all the differences, H_{Mg} desorption energies from both of these structures have the tendency to converge to the value of bulk rutile MgH_2 (0.67 eV/ H_2) with increasing MgH_2 layer thickness. This thickness dependence tends to be absent beyond a certain thickness.

It should be noted that for $\text{MgH}_2/\text{CrH}_2$ is exceptional. The formation energy of CrH_2 (+0.13 eV/ H_2) is much lower than that of MgH_2 . The hydrogen desorption energies in the sequence of H_{Cr} , H_{CrMg} , and H_{Mg} were also calculated. They are 0.04, 0.35 and 0.20 eV/ H_2 , respectively. The H_{Cr} desorption energy is nearly zero. This is consistent with the experimental finding that the hydrogen does not absorb in metal Cr at room temperature.³⁸ In fact, electrochemical measurements also revealed that due to the positive formation energy and small crystal lattice of CrH_2 , the hydrogen ab(de)sorption rates and capacity in $\text{Mg}_{80}\text{Cr}_{20}\text{H}_y$ thin films were much slower than those of $\text{Mg}_{80}\text{Ti}_{20}\text{H}_y$ and $\text{Mg}_{80}\text{Sc}_{20}\text{H}_y$.²⁷ A more stable metal hydride has to be added before the $\text{Mg}_x\text{Cr}_{1-x}\text{H}_2$ system can be used for hydrogen storage materials.

V. DISCUSSIONS

To understand the origin of the structural transformation as well as the tuned H_{Mg} desorption energies, H_{MgTM} and H_{TM} desorption energies were also calculated and are shown

together with that of H_{Mg} in Table II. As mentioned before, both the crystal structures of MgH_2 and of TMH_2 are deformed upon forming the multilayered structures. Comparing the lattice parameters and desorption energies of the two structures, one can directly see the relation between the structures and the energies [see also Fig. 3(b)]. On the one hand, the H_{Mg} desorption energies from $\text{MgH}_2(\text{rutile})/TMH_2(\text{fluorite})$ are larger than those from $\text{MgH}_2(\text{fluorite})/TMH_2(\text{fluorite})$ because rutile MgH_2 is more stable than fluorite MgH_2 . On the other hand, H_{TM} desorption energies from $\text{MgH}_2(\text{rutile})/TMH_2(\text{fluorite})$ are all smaller than those from $\text{MgH}_2(\text{fluorite})/TMH_2(\text{fluorite})$. This is because the crystal-lattice deformation of TMH_2 in $\text{MgH}_2(\text{rutile})/TMH_2(\text{fluorite})$ is larger than that in $\text{MgH}_2(\text{fluorite})/TMH_2(\text{fluorite})$. The larger the lattice difference between the multilayers and bulk TMH_2 , the larger the destabilization of $TM\text{-H}_2$ (see Tables I and II).

However, the thermodynamics of H_{MgTM} can be ambiguous because for $\text{MgH}_2(\text{rutile})/TMH_2(\text{fluorite})$ multilayers, the structure of the interface tends to change from rutilelike to fluoritelike upon dehydrogenation of the MgH_2 layers. More important is that H_{MgTM} has only a minor effect on the H_{Mg} desorption energies. Therefore, the structural transformation of MgH_2 between rutile and fluorite in the multilayers is due to the energy competition between the favorable rutile MgH_2 and the unfavorable structural deformation of TMH_2 . When the MgH_2 layer is thick, the rutile structure dominates and compensates the energy lost by the severe structural deformation of TMH_2 layer. On the other hand, when the MgH_2 layer is very thin, the rutile MgH_2 cannot do so. The rutile structure has to transform to a fluorite one which can minimize the energy lost by the structural deformation of the TMH_2 .

VI. CONCLUSIONS

The hydrogen-storage properties of MgH_2/TMH_2 multilayers have been investigated by DFT calculations. The structural transformation of the MgH_2 layer from rutile to fluorite with decreasing thickness of the MgH_2 layer has been confirmed. The transition points depend on the $TM\text{-H}_2$ bond energies: the more stable the $TM\text{-H}_2$, the easier the transformation. The calculated hydrogen desorption energies indicate that the Mg-H bond are profoundly destabilized in the $\text{MgH}_2(\text{fluorite})/TMH_2(\text{fluorite})$ multilayers. The structural deformation of the MgH_2 layer due to the strain induced by TMH_2 's is found to be responsible for the destabilization of the Mg-H: the more structural deformation, the more Mg-H destabilization.

¹L. Schlapbach and A. Züttel, *Nature (London)* **414**, 353 (2001).

²J. F. Stampfer, C. E. Holley, and J. F. Suttle, *J. Am. Chem. Soc.* **82**, 3504 (1960).

³W. Grochala and P. P. Edwards, *Chem. Rev.* **104**, 1283 (2004).

⁴B. Bogdanovic, K. Bohmhammel, B. Christ, A. Reiser, K. Schlichte, R. Vehlen, and U. Wolf, *J. Alloys Compd.* **282**, 84 (1999).

⁵R. Wagemans, J. H. van Lenthe, P. E. de Jong, A. J. van Dillen, and K. P. de Jong, *J. Am. Chem. Soc.* **127**, 16675 (2005).

⁶Z. G. Wu, M. D. Allendorf, and J. C. Grossman, *J. Am. Chem. Soc.* **131**, 13919 (2009).

⁷K. C. Kim, B. Dai, J. K. Johnson, and D. S. Sholl, *Nanotech.* **20**, 204001 (2009).

- ⁸P. Vajeeston, P. Ravindran, and H. Fjellvåg, *Nanotechnology* **19**, 275704 (2008).
- ⁹J. J. Liang, *Appl. Phys. A: Mater. Sci. Process.* **80**, 173 (2005).
- ¹⁰R. Varin, T. Czujko, C. Chiu, and Z. Wronski, *J. Alloys Compd.* **424**, 356 (2006).
- ¹¹W. Y. Li, C. S. Li, H. Ma, and J. Chen, *J. Am. Chem. Soc.* **129**, 6710 (2007).
- ¹²B. Bogdanović, *Int. J. Hydrogen Energy* **9**, 937 (1984).
- ¹³M. Y. Song, D. R. Mumm, S. N. Kwon, S. H. Hong, and J. S. Bae, *J. Alloys Compd.* **416**, 239 (2006).
- ¹⁴G. Barkhordarian, T. Klassen, and R. Bormann, *J. Phys. Chem. B* **110**, 11020 (2006).
- ¹⁵T. Vegge, L. S. Hedegaard-Jensen, J. Bonde, T. R. Munter, and J. K. Nørskov, *J. Alloys Compd.* **386**, 1 (2005).
- ¹⁶A. J. Du, S. C. Smith, X. D. Yao, and G. Q. Lu, *J. Phys. Chem. B* **110**, 21747 (2006).
- ¹⁷W. P. Kalisvaart and P. H. L. Notten, *J. Mater. Res.* **23**, 2179 (2008).
- ¹⁸R. A. H. Niessen and P. H. L. Notten, *Electrochem. Solid-State Lett.* **8**, A534 (2005).
- ¹⁹P. Vermeulen, R. A. H. Niessen, D. M. Borsa, B. Dam, R. Griessen, and P. H. L. Notten, *Electrochem. Solid-State Lett.* **9**, A520 (2006).
- ²⁰P. Vermeulen, R. A. H. Niessen, and P. H. L. Notten, *Electrochem. Commun.* **8**, 27 (2006).
- ²¹P. Vermeulen, P. C. J. Graat, H. J. Wondergem, and P. H. L. Notten, *Int. J. Hydrogen Energy* **33**, 5646 (2008).
- ²²D. M. Borsa, R. Gremaud, A. Baldi, H. Schreuders, J. H. Rector, B. Kooi, P. Vermeulen, P. H. L. Notten, B. Dam, and R. Griessen, *Phys. Rev. B* **75**, 205408 (2007).
- ²³G. Liang, J. Huot, S. Boily, A. V. Neste, and R. Schulz, *J. Alloys Compd.* **291**, 295 (1999); **292**, 247 (1999); **282**, 286 (1999).
- ²⁴B. Zahiri, C. T. Harrower, B. Shalchi-Amirkhiz, and D. Mitlin, *Appl. Phys. Lett.* **95**, 103114 (2009).
- ²⁵X. Tan, C. T. Harrower, B. Shalchi-Amirkhiz, and D. Mitlin, *Int. J. Hydrogen Energy* **34**, 7741 (2009).
- ²⁶J. Lu, Y. Choi, Z. Z. Fang, H. Y. Sohn, and E. Rönnebro, *J. Am. Chem. Soc.* **131**, 15843 (2009); **132**, 6616 (2010).
- ²⁷A. Baldi, M. Gonzalez-Silveira, V. Palmisano, B. Dam, and R. Griessen, *Phys. Rev. Lett.* **102**, 226102 (2009).
- ²⁸A. Baldi, G. K. Pálsson, M. Gonzalez-Silveira, H. Schreuders, M. Slaman, J. H. Rector, G. Krishnan, B. J. Kooi, G. S. Walker, M. W. Fay, B. Hjörvarsson, R. J. Wijngaarden, B. Dam, and R. Griessen, *Phys. Rev. B* **81**, 224203 (2010).
- ²⁹B. R. Pauw, W. P. Kalisvaart, S. X. Tao, M. T. M. Koper, A. P. J. Jansen, and P. H. L. Notten, *Acta Mater.* **56**, 2948 (2008).
- ³⁰S. Er, D. Tiwari, G. A. de Wijs, and G. Brocks, *Phys. Rev. B* **79**, 024105 (2009).
- ³¹G. Kresse and J. Furthmüller, *Phys. Rev. B* **54**, 11169 (1996).
- ³²G. Kresse and J. Furthmüller, *Comput. Mater. Sci.* **6**, 15 (1996).
- ³³G. Kresse and D. Joubert, *Phys. Rev. B* **59**, 1758 (1999).
- ³⁴J. P. Perdew, *Physica B: Condens. Matter* **172**, 1 (1991).
- ³⁵H. J. Monkhorst and J. D. Pack, *Phys. Rev. B* **13**, 5188 (1976).
- ³⁶H. Smithson, C. A. Marianetti, D. Morgan, A. Van der Ven, A. Predith, and G. Ceder, *Phys. Rev. B* **66**, 144107 (2002).
- ³⁷P. Villars, *Pearson's Handbook "Crystallographic Data for Intermetallic Phases"* (ASM International, Materials Park, OH, 1997).
- ³⁸E. Martin, *Arch. Eisenhuettenwes.* **3**, 407 (1929).